Acta Cryst. (1964). **17**, 1229

Evaluation of Truncation Methods for Accurate Centroid Lattice Parameter Determination*

BY J. TAYLOR, M. MACK AND W. PARRISH

Philips Laboratories, Irvington-on-Hudson, New York, U.S.A.

(*Received* 13 *September* 1963)

The centroid method provides a rational approach to the problem of the accurate determination of lattice parameters. The method requires (1) precise measurement of the line profiles, (2) calculation of the centroid, (3) correction of the centroid for aberrations, goniometer calibration, *etc.*, and (4) knowledge of the centroid of the incident spectral distribution. Four proposed methods for establishing finite limits by truncating a diffraction line profile are reviewed. The methods are evaluated from both a theoretical and practical viewpoint and the superiority of one of the methods is demonstrated. The effects of $K\beta$ lines, $K\alpha$ satellite lines and the background on the centroid are discussed. Lattice parameters of silicon and tungsten derived using both Fe $K\alpha$ and Cu $K\alpha$ radiations are given. The results are free of systematic error, and it appears that the centroid method can be used to obtain lattice parameters of greater accuracy than has heretofore been possible, provided accurate spectral centroid data can be obtained.

1. Introduction

The advantages of using centroids as measures of diffraction angles of X-ray powder diffraction profiles in order to permit corrections for systematic errors in accurate lattice parameter determinations has been recognized for some time (Parrish & Wilson, 1954). The theory has been described by Pike & Wilson (1959), Ladell, Parrish & Taylor (1959), and Umanskii, Kheiker & Zevin (1959). The necessity for properly accounting for systematic errors in precision lattice parameter determination was shown clearly in the recent I.U.Cr. project (Parrish, 1960).

The centroid method requires accurate measurements of the complete line profiles and obviously is not a simple experimental procedure. Since the tails decay rather slowly and overlap in substances with large unit-cell dimensions and low symmetry, the method is limited in its application with presently available equipment and techniques. Nevertheless the method provides a sound fundamental basis for the determination of accurate lattice parameters and therefore is of great interest. Although other measures of diffraction angles, such as the peak and mid-points of chords, do not lead to accurate or unique values (Parrish, Taylor & Mack, 1964), it might be possible to interpret such data in a better manner from our knowledge of the centroid method.

The practical and theoretical difficulties in determining centroids of complete line profiles have resulted in the proposal of four methods of truncating the profiles in such a way that their basic features are preserved and the difficulties avoided. The purpose of this paper is to evaluate these methods by applying them to the accurate lattice parameter determination of silicon and tungsten, using Cu $K\alpha$ and Fe $K\alpha$ radiation.

The application of each of the four truncation methods does not lead to the same centroid angle for a given powder line profile, nor to the same centroid wavelength for the incident spectral profile. The centroid method does not predict a unique centroid value, but rather requires that for a given truncation method to be valid, there must be a one-to-one correspondence between the centroids of the spectral and powder profiles (corrected for aberrations). This equivalence of the two centroids is essential to obtain the correct solution of the Bragg equation. Consequently, although certain aspects of the truncation methods are apparent from their application to powder line profiles, a complete evaluation requires that the spectral profiles must be treated in the same manner as the diffractometer profiles. Hence we have also applied the truncation methods to Cu $K\alpha$ and Fe $K\alpha$ two-crystal spectrometer spectral profiles kindly prepared for this analysis by Prof. J. A. Bearden (Bearden, 1960). The data on these centroid wavelengths have recently been published (Mack, Parrish & Taylor, 1964) and are used in this paper*.

2. Truncation methods

For convenience, we shall indicate the four truncation methods as *A*, *B*, *C*, and *D*. To simplify the descrip-

* Sponsored in part by U.S. Air Force Office of Scientific Research under Contract No. AF49(638)-620. Presented in part at I.U.Cr., Rome, Italy, Sept. 1963, Paper No. 18(ii).4.

* Most published X-ray wavelengths are peak values (DuMond, Cohen & McNish, 1962). The Bearden 1960 curves were measured far out into the tail regions to permit calculations of the centroid wavelengths.

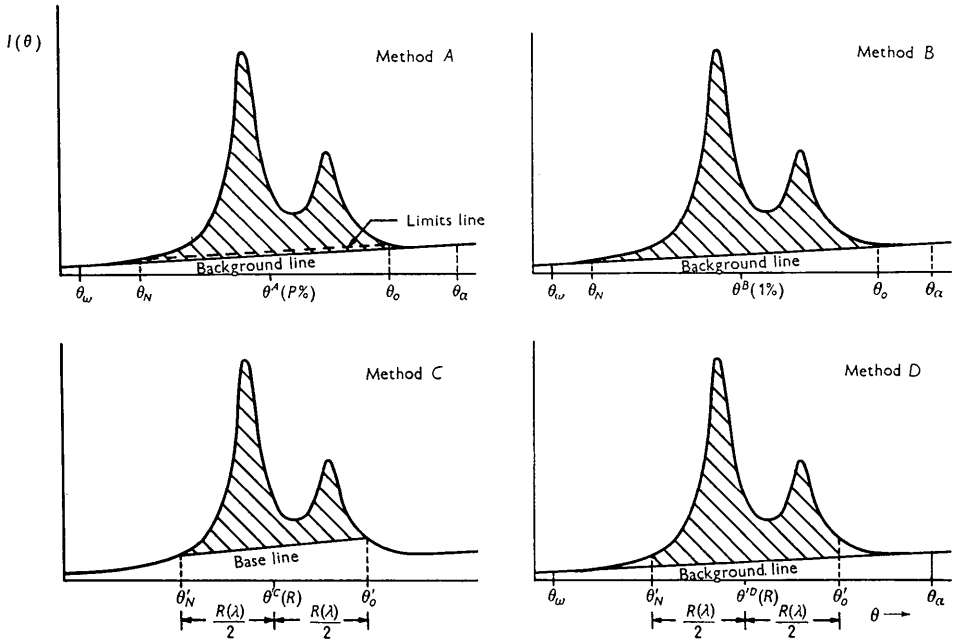

Fig. 1. Schematic illustration of four methods proposed to truncate profiles for centroid determination. The striped areas indicate the truncated profile. Method *A* (Ladell, Parrish & Taylor, 1959); Method *B* (Zevin, Umanskii, Kheiker & Panchenko, 1962); Method *C* (Pike & Wilson, 1959); Method *D* (Taylor, Mack & Parrish, 1963).

tions, the truncations are illustrated schematically in Fig. 1 for a powder line profile. The centroids will be identified by adding a superscript *A*, *B*, *C*, or *D* to indicate the method, and parentheses to indicate the basis for the choice of limits. For example, θ^A (90%) refers to method *A* using 90% of the integrated intensity to establish the limits line, and θ^D (0·014 kX) refers to method *D* using an angular range which corresponds to a wavelength range of 0·014 kX (as explained below). The centroids of the spectral distributions are indicated in the same manner with λ substituted for θ.

In all methods the centroid was calculated by numerical integration from the relation,

$$\sum_{j=0}^{N} \theta_j[I(\theta_j)-L(\theta_j)] \Big/ \sum_{j=0}^{N} [I(\theta_j)-L(\theta_j)] \qquad (1)$$

where $\theta_j=\theta_{j-1}+\Delta\theta$, $I(\theta)$ is the observed line profile, θ_0 and θ_N are the truncation limits, and $L(\theta)$ is the background or 'base' line. We refer to the portion of the profile lying between the truncation limits and above the line $L(\theta)$ as the truncated profile (the hatched areas of Fig. 1). The criteria for defining the truncated profile for each of the four truncation methods are outlined below. The experimental procedures for determining $I(\theta)$ and $L(\theta)$ are discussed in § 3. The following description of the methods deals with how they were applied to obtain the centroid values. The original papers should be consulted for discussions of the theoretical foundations and the variations possible within the framework of a given method.

2.1. *Description of truncation methods*

Method A. $L(\theta)$ is the conventional background $B(\theta)$, determined as described in § 3, and the limits θ_0 and θ_N satisfy the following criteria: (1) $f(\theta_0)=f(\theta_N)$, where $f(\theta)=I(\theta)-B(\theta)$, and (2) the area above a 'limits line' established by joining the point θ_0, $I(\theta_0)$ and the point θ_N, $I(\theta_N)$ is a selected fraction (P%) of the integrated intensity. In the original proposal of the method (Ladell, Parrish & Taylor, 1959), it was suggested that setting the value of P at 90% was a satisfactory compromise for including virtually all of the aberration effects but excluding small portions of the tails which are difficult to measure because of the low signal to background ratio. In applying *A*, centroids were calculated with $P=85$, 88, 90, 92 and 94% to observe experimentally the dependence of centroids on truncation limits. At $P=85$%, part of the aberration is sometimes excluded; at $P=94$%, the tails become troublesome. The intermediate values of P were tried to assess the sensitivity of the centroid to small deviations from the 90% criterion which could result, for example, from a slight indeterminacy in the assignment of the background. The corrected centroid is found by adding Δ_{Ab} to the calculated centroid. Δ_{Ab} is the algebraic sum of the centroid corrections resulting from instrumental aberrations (*e.g.* flat specimen and axial divergence),

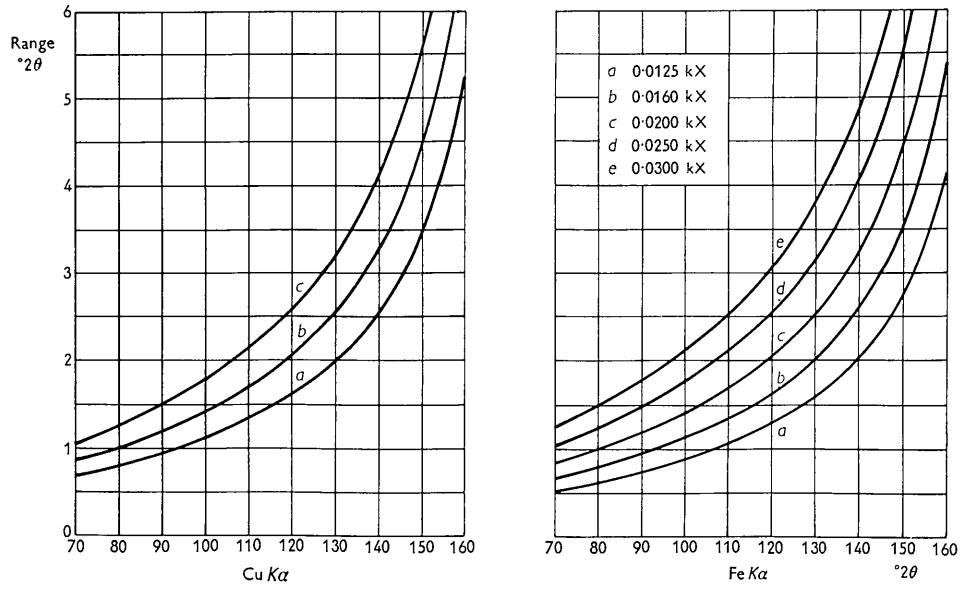

Fig. 2. Angular range corresponding to various wavelength ranges R as a function of diffraction angle for Cu $K\alpha$ and Fe $K\alpha$ radiations.

specimen aberrations (*e.g.* transparency and displacement), and the goniometer angle corrections (zero angle and gear calibrations). Δ_{Ab} also includes the Lorentz, polarization and dispersion corrections which we shall call Δ_L.

Method B. $L(\theta)$ is defined as in method A, and the limits θ_0 and θ_N satisfy the criterion $f(\theta_0)=f(\theta_N)=0{\cdot}01[f(\theta)]_{\max}$ (Zevin, Umanskii, Kheiker & Panchenko, 1961). Although the authors proposed the method for $K\beta$ lines, we have applied it to $K\alpha$ lines for purposes of comparison with the other methods. Using limits at 1% of the $K\alpha_1$ peak intensity, the truncated profile defined by B was found to be the same as that for A with $P \approx 92\%$. Slightly varying the 1% criterion has the same effect on the limits as varying the value of P in method A. Since comments on A apply equally to B, and the results for A (92%) are the same as those for B (1%), no further discussion of B will be given.

Method C. $L(\theta)$ is the *base line* (not the same as $B(\theta)$) established by joining the point θ_0', $I(\theta_0')$ and the point θ_N', $I(\theta_N')$ (Pike & Wilson, 1959). The truncation limits θ_0' and θ_N' lie on either side of the $K\alpha$ doublet and satisfy the following criteria: (1) the range $\theta_0'-\theta_N'$ is large compared with the width of the aberration functions but does not include the β-filter absorption edge, and (2) equivalent wavelength ranges R are used in computing the centroid of the observed powder line profile θ'^C and the incident spectral profile, *i.e.* θ_0' and θ_N', when corrected for aberrations (to θ_0 and θ_N) correspond to λ_0 and λ_N on the spectral profile (see equation 2). By a series of successive approximations a value of d_{hkl} is found which is used to transform the limits and centroid of the truncated spectral profile to equivalent points on the observed powder profile by the equations

$$\theta_0' = \theta_0-(\Delta_{Ab}-\Delta_L)=[\sin^{-1}(\lambda_0/2d)]-(\Delta_{Ab}-\Delta_L)$$
$$\theta_N'=\theta_N-(\Delta_{Ab}-\Delta_L)=[\sin^{-1}(\lambda_N/2d)]-(\Delta_{Ab}-\Delta_L)\,. \quad (2)$$

The correction Δ_L is taken into account at the final step* in which the corrected centroid (*i.e.* the powder profile centroid which corresponds to the spectral centroid) is found from

$$\theta^C=\theta'^C+\Delta_{Ab}\,. \quad (3)$$

Pike & Wilson discuss the fact that the equivalence between points on the powder line and spectral profile is not exact because of the 'smearing' effect of the aberrations but point out that the error is negligible if the range is sufficiently large.

The above description is essentially the 'unsimplified procedure' of Pike & Wilson. Their criteria allow rather wide latitude in the choice of limits. From the innumerable possibilities we have considered only the particular case in which the limits are symmetrical (on a wavelength scale) about the centroid. This choice also enabled us to evaluate their 'simplified procedure' for which symmetrical limits are a requirement. Thus we have imposed a third criterion which applies only to the symmetrical case, *viz.* (3) $\lambda_0-\lambda^C=\lambda^C-\lambda_N=R/2$. The angular range which corresponds to a given wavelength range is plotted as a

* The correction Δ_{Ab}, rather than $\Delta_{Ab}-\Delta_L$, is used in equation (2) in the Pike–Wilson treatment. However, at high angles where Δ_L is large, the successive approximation will not converge if this is done.

function of diffraction angle in Fig. 2 for Cu $K\alpha$ and Fe $K\alpha$ radiations.

Method D. $L(\theta)$ is defined as in method A, and the limits θ'_0 and θ'_γ satisfy the same criteria as in method C, incuding the third requirement of symmetrical limits, and are found as in C from equations (2) (Taylor, Mack & Parrish, 1963). To establish the appropriate range, an approximate range for each reflection is selected by studying a preliminary scan. Initial limits are chosen which are roughly symmetrical about the approximate centroid at points where the intensities $f(\theta)$ are about 1% of the $K\alpha_1$ peak intensity. The wavelength range is found from the angular range by use of the appropriate curve in Fig. 2. This approximate range is then used for the centroid determination of the carefully measured profile and modified if necessary in subsequent calculations. For a given radiation, the angular range required increases with increasing Bragg angle, but the wavelength range decreases. For example, for Cu $K\alpha$ radiation with our experimental parameters, a range of 0·0145 kX (5.9° 2θ) was appropriate for the Si 444 profile at 159° 2θ and 0·0250 kX (1.8° 2θ) for Si 422 at 88° 2θ. For purposes of studying the effect of range on the centroid, ranges of from 0·0125 kX to 0·0300 kX were used.

The corrected centroid is found from equation (3). Thus for D, the background is defined as in A, but the truncation limits and centroid are found as in C.

2.2. *Range requirements*

The width and shape of a powder diffractometer profile, and hence the magnitude of the range required, depend on the combined effect of the incident spectral distribution (asymmetry, width, doublet

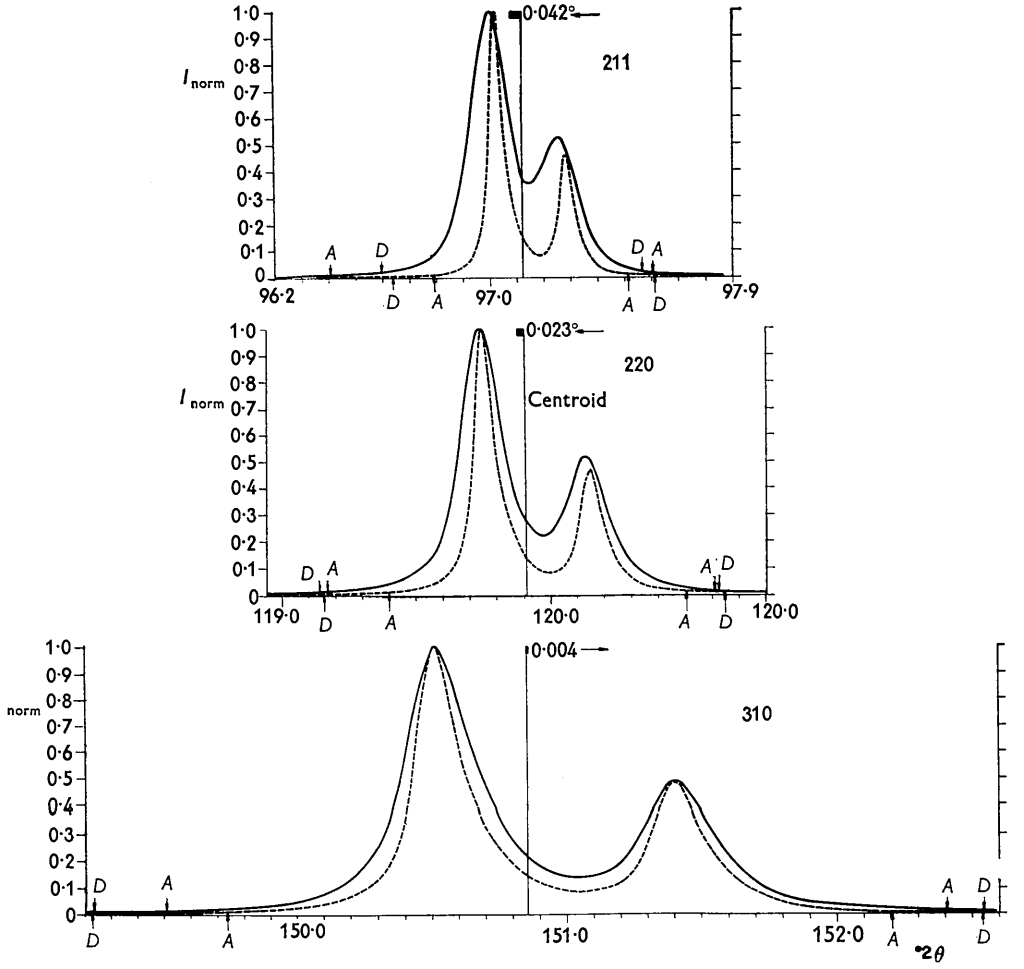

Fig. 3. Diffractometer powder profiles (solid curves) and dispersed two-crystal spectrometer profiles (dashed curves). Powder profiles obtained with tungsten specimen, Fe $K\alpha$ radiation, angular aperture $\alpha = 3{\cdot}89°$, receiving slit 0·10°(2θ). Dispersed profiles obtained by dispersing Bearden 1960 Fe $K\alpha$ spectral curve to appropriate angles for tungsten 211 reflection (upper curve), 220 reflection (middle curve) and 310 reflection (lower curve). Vertical arrows marked A indicate Method A (90%) truncation limits, vertical arrows marked D indicate Method D (0·0145kX) truncation limits, horizontal arrows indicate the direction in which the aberrations shift the incident spectral profile.

separation, *etc.*) and the aberration functions at the particular reflection angle. The spectral profile is dominant at high angles and the convolution of the aberration distributions at lower angles, but in general these two factors do not compensate. Thus neither a constant wavelength range nor a constant angular range can be used for all reflections. Fig. 3 illustrates the relative contributions of the incident spectral distribution and the aberration functions at various reflection angles. The solid line profiles in Fig. 3 are experimentally observed diffractometer profiles of tungsten powder; Fe $K\alpha$ radiation was used, the background has been subtracted, and the angle scale has been adjusted for the goniometer angle correction. The dashed line profiles were plotted by dispersing the Bearden Fe $K\alpha$ two-crystal spectrometer profile to the appropriate angle by means of the Bragg equation. They approximate the dispersed incident spectral profiles, *i.e.* 'ideal' profiles which would be obtained with a perfect specimen and an aberrationless instrument. The lattice parameter used for the transformation was the experimental value obtained for tungsten, $a=3{\cdot}15898$ kX (see Table 6(*a*)), and each ordinate was adjusted for the Lorentz and polarization effect. The vertical line on each profile indicates the corrected (except for Δ_L) centroid angle of the diffractometer and dispersed spectral profiles. The sum of the first moments of the aberration functions, except for Lorentz–polarization and dispersion, and the sense of the displacement are indicated on the figure for each reflection. The method *A* 90% limits and the method *D* 0·0145 kX limits for the diffractometer profiles are indicated by arrows pointing down, and for the spectral profile by arrows pointing up.

Since the range is partially dependent on the spectral distribution, different radiations will require different ranges for a given reflection angle. For example, at a given angle, a reflection obtained with Fe $K\alpha$ will have greater width and asymmetry than one obtained with Cu $K\alpha$, and to include the same features a larger wavelength range will be necessary for Fe $K\alpha$ although the angular range is about the same.

3. Measurement of powder line profiles

The centroid calculations for all four truncation methods are amenable to electronic digital computer techniques, which greatly reduce the time required compared with manual methods. The profiles analyzed for the comparison given here were measured by automatically step-scanning with the diffractometer through equal angular increments of 0·01 to 0·05° (2θ) depending on the breadth of the profile. The intensity was detected by a scintillation counter with pulse amplitude discrimination, counting for a fixed time at each step (Parrish, 1962*a*, *b*). The specimen was maintained at a constant temperature of 38·2 °C. In our experimental arrangement (which will be described in detail in another paper) the intensity data were punched directly on tape which was used as the input for a Bendix G15 computer. For each profile, the centroids were computed by inserting the appropriate computer program and input control data in conjunction with the intensity data tape. Each reflection considered was measured in its entirety several times; the various truncation methods were applied to the same set of intensity data, and for each method several ranges were used. This procedure was followed to permit comparison of the four methods. In practice, only one method would be used and the profile measurement technique would be tailored to the method selected. Certain features of the profile which assume varying degrees of importance in each of the truncation methods are discussed below.

Method A: The entire profile must be measured and the integrated intensity determined to an accuracy of about 1%. To speed up the profile measurement, a shorter counting time interval was used in the extreme tail regions. These areas are not included in the truncated profile and contribute only a small amount (0·5 to 2%) to the integrated intensity. The counting statistical errors, though large, are random and hence tend to cancel out and have little effect on the integrated intensity.

Although the truncation limits lie in the region in which the longer time interval is used, the intensities here are still relatively weak, and hence the counting statistical errors are considerable. The limits θ_0 and θ_N are established on the basis of equal intensities, and large statistical fluctuations cannot be tolerated as they could give rise to spurious choices of limits. To avoid this difficulty a smoothing process was included in the computer program which consisted in using a moving average of several steps to recalculate the intensities in the regions of the truncation limits. The validity of this procedure has been verified by the good agreement between a smoothed region and the same region measured with higher precision (100 sec counting time at each step). Once θ_0 and θ_N had been determined, the observed $f(\theta)$ values were used in the centroid calculation. It should be noted that for method *B* the integrated intensity is not needed, but the smoothing is still necessary.

The background line must be established to a precision of about 1%. This was accomplished by counting for the necessary length of time at θ_α and θ_ω, which lie well beyond the points where the tails of the profile merge into the background. The angles θ_α and θ_ω were varied slightly to determine if they were sufficiently far from the profile — the intensities should fit a straight line function.

In succeeding measurements of the same reflection it was necessary to repeat the entire procedure. We found the reproducibility of methods *A* and *B* truncation limits and centroids to be somewhat poorer than for methods *C* or *D*, primarily because of the dependence of the truncation limits on weak intensities.

Method C: Neither the integrated intensity nor the

background level is required, but the intensities $I(\theta_0')$ and $I(\theta_N')$ (see Fig. 1(*c*)) must be accurately determined, since they establish the base line. We used the same smoothing process as described for the method *A* limits. Pike & Wilson (1959) recommended counting these intensities for long time intervals, but this procedure was not practical for our comparison. The good reproducibility of the method *C* centroids indicated that no significant errors had been introduced by using the smoothing process rather than longer counting times. Our procedure entailed applying all the methods to the same set of profile intensity data. If only method *C* had been used, once the limits and the appropriate range for a given reflection had been determined, subsequent measurements of the same reflection could have been confined to the range defined by these limits, and long time intervals could be used for measuring $I(\theta_0')$ and $I(\theta_N')$.

To determine method *C* limits an exact knowledge of the centroid wavelength is not required. An approximate value of λ^C, such as the weighted mean of the α_1 and α_2 peak wavelengths, is adequate to find λ_0 and λ_N for use in equations (2). Hence refinements in the knowledge of the spectral distributions will generally have no effect on the calculated powder *centroid* values. To find d_{hkl}, however, λ^C for the same range as that used in determining θ^C must be accurately known. For this purpose, accurate knowledge of the entire spectral distribution is essential in order to determine λ^C for a series of ranges. It is not feasible either practically or theoretically to use the same range for all reflections.

Method D: The integrated intensity is not required and the intensities at the limits have no special significance. However, the background line must be accurately determined and is established as described in this section for method *A*. Pre-selection of limits after a trial measurement of the profile to establish the range is possible for *D* as well as *C*. The relationship to spectral information is the same for *D* as for *C*.

4. Variation of centroid with range

All reflections of tungsten and silicon occurring in the region from 80° to 160° (2θ) were measured with both Cu and Fe radiation. Each reflection was measured several times; the observed mean powder centroids, corrected only for the goniometer angle calibration, are shown as a function of range of integration in Fig. 4 for some of the silicon reflections. For method *A* the range (the abscissa scale) is determined by the percentage *P*, and for methods *C* and *D* by the symmetrical wavelength range *R*. The spectral centroids obtained by similar truncations of the Bearden two-crystal spectrometer profiles are plotted along the bottom.

The variation of the centroid with truncation method and range is directly related to the truncated profile defined by each method and is dependent on the extent to which the $K\alpha$ satellite group and the tails of the aberration distributions contribute moments in the calculation of the centroid.

Fig. 5 shows the tail regions of the tungsten 211 powder reflection and the Bearden spectral profile dispersed to the same angle. The ordinate scale has been expanded to emphasize the relation between the truncated powder and spectral profiles. The profiles were obtained as described for Fig. 3, but each spectral

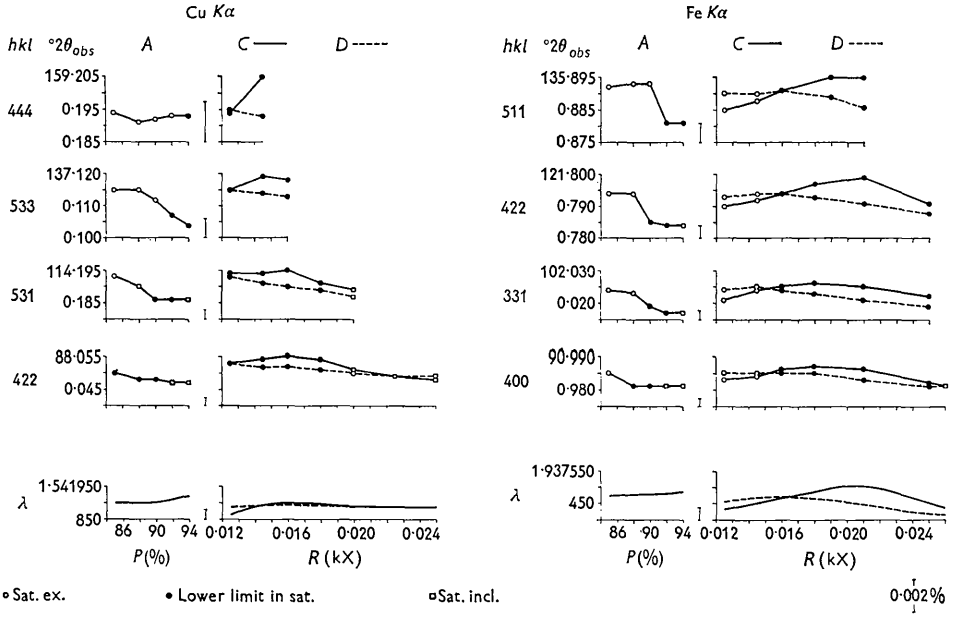

Fig. 4. Plot of observed mean centroid values obtained by methods *A*, *C*, and *D* *versus* range of integration for some of the back reflection lines of silicon (above) and corresponding centroid wavelengths of the Bearden spectral profiles (bottom).

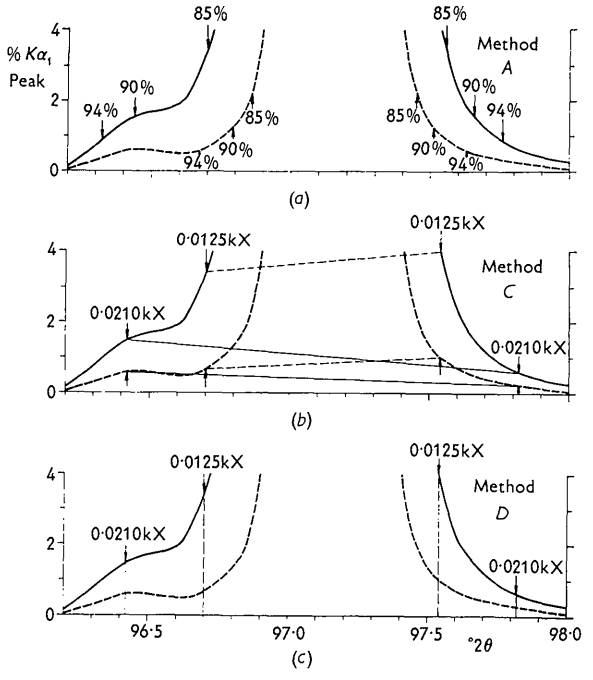

Fig. 5. Tail regions of tungsten 211 diffractometer profile (solid curves) and dispersed Bearden spectral profile (dashed curves) shown in Fig. 3. (*a*) Method *A* truncation limits for $P=85$, 90, and 94% are indicated for the powder profile by arrows pointing down and for the spectral profile by arrows pointing up; (*b*) Method *C* truncation limits are indicated as in the upper curve, and the base lines for the powder and spectral profiles are drawn for $R=0{\cdot}0125$ kX (dotted lines) and for $R=0{\cdot}0210$ kX (solid lines); (*c*) Method *D* truncation limits for $R=0{\cdot}0125$ kX and $R=0{\cdot}0210$ kX are indicated. The required equivalence of the truncated spectral and powder profiles can be seen.

profile has been translated by an amount equal to the centroid correction for the reflection. This procedure results in the superposition of the spectral and powder profile limits for methods *C* and *D* but not for method *A*; the effect of this lack of equivalence between spectral and powder profiles for method *A* is considered below. The broad 'hump' in the low angle tails is due to the $K\alpha$ satellite group, which contributes a significant, though small, moment to the total moment. For shorter ranges, the truncated powder profile excludes the satellites and aberration tails, whereas these are included in longer ranges. The net effect is to cause the powder centroids to decrease with increasing range in each method.

For a given range, the extent to which the aberration tails are excluded from the truncated profile is Bragg angle dependent because the aberrations decrease with increasing Bragg angle (up to about 150° 2θ). A comparison of the dispersed spectral and powder profile tails indicates qualitatively how much of the aberration tails have been excluded. The Bragg angle dependence may be seen by comparing truncations for the three different reflections shown in Fig. 5(*c*), the tungsten 211 reflection (97·1° 2θ), and the plots in Fig. 6, which are the tails of method *D* truncated profiles of the tungsten 220 reflection (119·9° 2θ) and the tungsten 310 reflection (150·9° 2θ).

If the truncated spectral and powder profiles are equivalent, the variation with range of the powder centroids for a given reflection will parallel that of the spectral centroids. To facilitate comparison of the powder and spectral centroid plots in Fig. 4, a vertical line is shown on each plot. This line represents the angular spread in each ordinate scale corresponding to a wavelength spread of one part in 50,000 (0·002%).

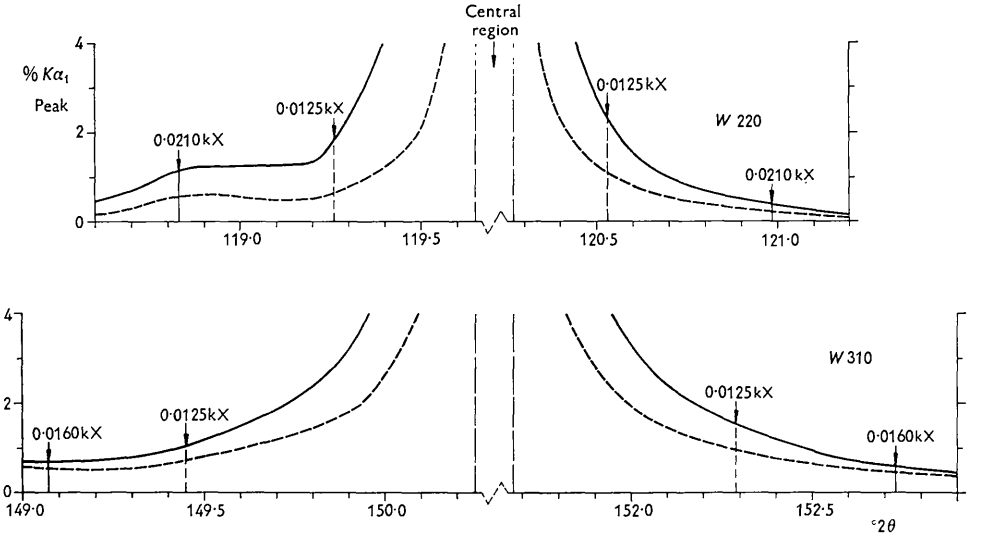

Fig. 6. Tail regions of the tungsten 220 profiles (top) and 310 profiles (bottom) shown in Fig. 3. The solid curves are the diffractometer profiles, the dashed curves are the dispersed Bearden spectral profile and the method *D* truncation is indicated. These curves, together with the 211 reflection (Fig. 5(*c*)), illustrate that for a given range the relative contributions of the spectral and aberration distributions to the intensities at the truncation limits are a function of Bragg angle.

The inconsistency of the variation of centroid with range in method A is discussed in § 5.

5. Effect of the $K\alpha$ satellite group

The $K\alpha$ satellite group is readily apparent in the precise line profiles measured for centroid determination. A detailed analysis of the satellites and their effect on powder line centroids obtained by the various truncation methods has been given elsewhere (Parrish, Mack & Taylor, 1963). Although the presence of the satellite group is a complicating factor, it serves as an internal check on the equivalence of the truncated powder and spectral profiles since its position and relative intensity are known. The satellite group is a salient feature of second order magnitude; any truncation method should be sensitive to a feature of this kind in order to be acceptable. The centroid values in Fig. 4 are coded to indicate the position of the satellite group relative to the truncated profile; open circles indicate that the satellite group was excluded from the truncated profile, squares that it was included and solid circles that it was partially included.

Method A: In general, the complete inclusion of the satellites within the truncated profile occurs at lower values of P, the lower the reflection angle. However, the truncated spectral profile completely excludes the satellites for all values of P considered (Fig. 5(*a*)). Thus the required equivalence between the spectral and powder line profiles is not realized in method A. It should be noted that the theoretical development of method A (Ladell, Parrish & Taylor, 1959) contained the assumption that the tails decreased monotonically and the presence of the satellite group negates this assumption.

Method C: To circumvent the difficulties involved in determining the 'true' background line, a base line established by a 'horizontal' truncation is used rather than the conventional background line. The slope of the base line (Fig. 5(*b*)) is considerably influenced by relatively minor features in the tails, such as the satellite group, and the centroid is concomitantly affected. Since equivalence is presumed to be maintained between the truncated powder and spectral profiles and the satellites are included or excluded in both, depending on the range, it might be supposed that the satellites would not be a source of difficulty. However, the artificial nature of the horizontal truncation, while not evident in powder diffractometer profiles, is clearly illustrated in two-crystal spectrometer profiles in which the background is low and well-defined. Furthermore, in practice, the spectral centroids for ranges in which the lower limit lies in the satellite region are extremely sensitive to variations in the slope of the base line. This sensitivity requires the spectral tails to be measured with very high accuracy. These problems have been discussed in detail (Mack, Parrish & Taylor, 1964). It is not possible to avoid this difficulty by taking a range which excludes the satellites, because such a range when applied to lower angle powder line profiles would exclude part of the aberrations.

The 'simplified procedure' of Pike & Wilson, which was proposed for use on profiles in the region from 60° to 140° (2θ), is based on the assumption that the tails of the powder and spectral profiles are monotonic decreasing functions out to the β-filter edge, as was assumed in method A. The authors predicted that the centroid would approach an asymptotic value as the range was increased. The presence of the satellite group violates this assumption and no asymptotic value is realized experimentally. For a given reflection the powder centroids tend to level off in the intermediate ranges and then decrease, but for the spectral profiles the centroid varies continuously for the ranges studied (see Fig. 4).

Method D: In this method, the presence of the $K\alpha$ satellite group does not cause difficulties. The minor effect of the satellite group on the centroid is the same for both the powder line and spectral profile. The observed shift in the centroid caused by the inclusion of the satellite group in the truncated powder line profile is equal to the amount predicted by calculating the moment exerted by the satellite group from its known position and relative intensity (Parrish, Mack & Taylor, 1963). Thus the decrease in centroid values with increasing range in method D is accounted for by the effect of the satellites.

A further advantage of D is the relative insensitivity of the spectral centroids to the accuracy of the tail regions of the spectral profiles. Small errors in these regions do not exert the disproportionate effect observed for method C.

6. Effect of $K\beta$ interferences

A suitable $K\beta$ filter will not completely eliminate $K\beta$ reflections and the stronger ones are readily apparent in precisely measured patterns. If the truncation limits for a given profile are such as to include a $K\beta$ line from another set of planes, a correction must be made since the β line is not a factor in the corresponding spectral centroid. The moment contributed by an interfering β line can be calculated to a first order approximation from a knowledge of its position and intensity. The intensity can be found indirectly from the relative intensities of the unfiltered $K\alpha:K\beta$ and the filter attenuation factors for $K\alpha$ and $K\beta$. Should the interfering β line fall in a tail region, considerations similar to the effect of the satellites would apply. In the analysis of the silicon and tungsten profiles given later, corrections to the centroids for β interferences have been made where appropriate. The pertinent data are given in Table 1.

Table 1. *Data for Kβ interferences*

Main line, $K\alpha_{1,2}$		Interf. line, $K\beta$			Cent. shift if $K\beta$ incl.	
hkl	Appr. cent. (°2θ)	*hkl*	Appr. peak (°2θ)	$I_\beta/I_{\alpha_{1+2}}$ (%)	(°2θ)	Remarks*
			(*a*) Silicon, Cu $K\alpha$			
444	159·34	553, 731	159·96	1·04	+0·006	Same shift in all methods
620	127·84	444	125·37	0·20	−0·005	Not included in any method
531	114·33	533	114·49	0·22	≈0	Included in all methods
440	106·92	620	108·41	0·67	+0·010	Not included in any method
511, 333	95·13	440	93·03	0·35	−0·007	Not included in any method
			(*b*) Silicon, Fe $K\alpha$			
400	91·53	331	90·15	1·05	−0·014	Not included in any method
			(*c*) Tungsten, Cu $K\alpha$			
310	100·83	222	99·34	0·01	≈0	Not included in any method
220	87·16	310	88·21	0·05	+0·001	Not included in any method
			(*d*) Tungsten, Fe $K\alpha$			
310	151·40	222	148·51	0·24	−0·007	Not included in any method

* The integrated intensity in Method *A* would be slightly high because of the contribution of the Kβ line.

7. Effect of background

In defining the background line $B(\theta)$ for centroid determinations, the intensities at both ends of the profile were established by accurate measurements as described earlier. The background line usually had a small slope which was assumed to vary linearly across the profile. There is some experimental evidence that the observed background is higher than the 'true' background because of overlapping tails even when the reflections are comparatively widely separated (Warren, 1959). Wilson (1962*a*) states that if the variance is not linear with range R, the measured background level is probably in error. In one case (Wilson, 1962*b*) an analysis of the variance indicated the true background was about two-thirds of the observed background.

The spectral composition of the background and its possible variation across the profile are not known accurately. An analysis of the spectral composition of the observed background in X-ray powder patterns of non-fluorescent specimens indicated that most of the background consisted of scattered characteristic radiation for the conditions employed in this study, *viz.* NaI.Tl scintillation counter with pulse amplitude discrimination (Parrish & Kohler, 1956). The ratio of scattered continuous to characteristic radiation was found to vary with diffraction angle and specimen. It is evident that the spectral composition of the powder diffractometer background is different from that of the two-crystal spectrometer background, but owing to the absence of quantitative data we have not taken this factor into consideration. Moreover, we have made no attempt to subtract the contribution of thermal diffuse scattering (Chipman & Paskin, 1959).

Method A: As long as the observed background is parallel to the true background, taking too high a background level is tantamount to using a smaller value of P for the limits line criterion. This can be visualized by translating the P scale of the plots in Fig. 4 for method *A*. The P scale for the spectral plot (bottom of Fig. 4) would be affected to a much smaller degree because of the different background composition and the inherently greater peak to background ratio of two-crystal spectrometer curves.

Method C: The differing composition of the powder line and spectral backgrounds and the consequent lack of identity between them, coupled with the 'horizontal' truncation which defines the base line (Fig. 1(*c*)), makes it extremely difficult to assess the effect of background on the equivalence of the centroids of the truncated powder line and spectral profiles. We have attempted no analysis along these lines other than to recognize the complexities involved.

Method D: The symmetrical limits criterion makes the centroid value of the truncated profile insensitive to departures of the observed background level from the true background, provided the two are parallel. The additional moments which are neglected by taking too high a background level are the same on either side of the centroid and cancel out.

8. Corrections

The displacement and distortion of observed X-ray diffractometer profiles caused by goniometer errors and geometrical and physical aberrations result in errors in the observed centroids for which corrections must be made (Wilson, 1963; Parrish, 1962*a*). A brief

Table 2. *Centroid corrections in °2θ for silicon and tungsten*

		Gon. Corr.		Aberration Corrs.									
								Δ_L, Methods C and D R (kX)			Sum of aberr. corrs. R (kX)		
hkl	Approx. $2\theta°$	Zero angle	Gon. gear calib.	Flat sp. $\alpha = 3{\cdot}89°$	Axial div. $\delta = 4{\cdot}5°$	Transp. $0{\cdot}55\varrho_{sol}$	Spec. displ.	0·0125	0·0200	0·0280	0·0125	0·0200	0·0280
						(*a*) Silicon, Cu $K\alpha$							
444	159·2	−0·138	0	+0·0081	−0·0243	+0·0074	0		−0·0518			−0·061	
533	137·1	−0·138	+0·002	+0·0173	−0·0094	+0·0142	0		−0·0058			+0·016	
620	127·7	−0·138	+0·001	+0·0216	−0·0063	+0·0165	0		−0·0030			+0·029	
531	114·2	−0·138	+0·001	+0·0285	−0·0030	+0·0190	0		−0·0011			+0·043	
440	106·8	−0·138	+0·002	+0·0327	−0·0014	+0·0199	0		−0·0006			+0·062	
511	95·0	−0·138	+0·004	+0·0403	+0·0009	+0·0207	0		0			+0·062	
422	88·1	−0·138	+0·005	+0·0455	+0·0023	+0·0208	0		+0·0001			+0·069	
						(*b*) Silicon, Fe $K\alpha$							
511	135·9	−0·545	+0·002	+0·0178	−0·0089	+0·0075	0	−0·0035	−0·0044	−0·0052	+0·013	+0·012	+0·011
422	121·8	−0·545	+0·001	+0·0245	−0·0048	+0·0092	0	−0·0013	−0·0016	−0·0020	+0·028	+0·027	+0·027
331	102·0	−0·545	+0·003	+0·0356	−0·0005	+0·0106	0	−0·0002	−0·0003	−0·0003	+0·046	+0·045	+0·045
400	91·0	−0·545	+0·005	+0·0433	+0·0017	+0·0108	0	0	+0·0001	+0·0001	+0·056	+0·056	+0·056
311	72·5	−0·545	+0·006	+0·0601	+0·0055	+0·0103	0	+0·0002	+0·0002	+0·0003	+0·076	+0·076	+0·076
						(*c*) Tungsten, Cu $K\alpha$							
400	153·9	−0·132	0	+0·0102	−0·0187	+0·0004	+0·0008		−0·0265			−0·034	
321	131·3	−0·132	+0·002	+0·0199	−0·0074	+0·0007	+0·0014		−0·0039			+0·011	
222	115·0	−0·132	+0·001	+0·0280	−0·0032	+0·0008	+0·0018		−0·0012			+0·026	
310	100·7	−0·132	+0·003	+0·0365	−0·0002	+0·0009	+0·0022		−0·0003			+0·039	
220	87·0	−0·132	+0·005	+0·0464	+0·0025	+0·0009	+0·0025		+0·0002			+0·053	
						(*d*) Tungsten, Fe $K\alpha$							
310	150·9	−0·542	0	+0·0114	−0·0163	+0·0002	+0·0009	−0·0125	−0·0156	−0·0186	−0·016	−0·019	−0·022
220	119·9	−0·542	+0·001	+0·0255	−0·0043	+0·0004	+0·0017	−0·0012	−0·0014	−0·0017	+0·022	+0·022	+0·022
211	97·1	−0·542	+0·004	+0·0389	+0·0005	+0·0005	+0·0022	−0·0001	−0·0001	−0·0001	+0·042	+0·042	+0·042
200	75·4	−0·542	+0·006	+0·0569	+0·0049	+0·0005	+0·0027	+0·0002	+0·0002	+0·0003	+0·065	+0·065	+0·065

discussion of each correction and the appropriate references are given below. The values of the corrections for silicon and tungsten back reflection centroids for Cu $K\alpha$ and Fe $K\alpha$ radiations are given in Table 2 for the experimental factors described in this paper. The goniometer corrections were determined experimentally and the aberration corrections were calculated for the experimental conditions used. These corrections were applied to the centroids obtained by all truncation methods and for all ranges, but it should be noted that use of the full aberration corrections is not valid if a truncated profile does not include virtually all of the aberration function. A plot of the aberration corrections as a function of 2θ for Cu $K\alpha$ radiation is shown in Fig. 7 for $2\theta = 70°$ to 170°. Perhaps the best overall test of the validity of the corrections is the elimination of systematic errors in the lattice parameter results presented in § 9.

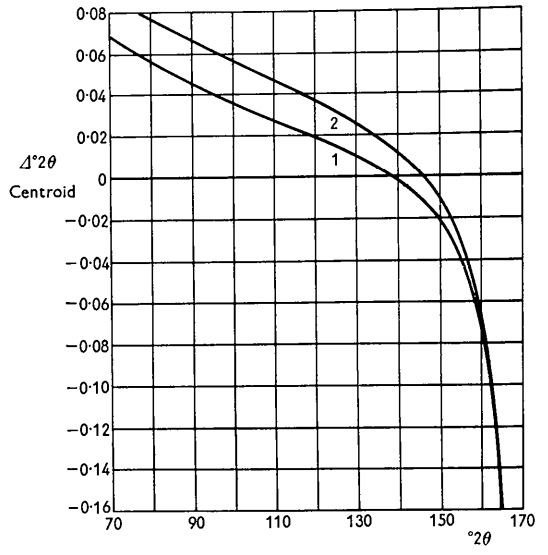

Fig. 7. Total aberration corrections as a function of diffraction angle for Cu $K\alpha$ radiation, goniometer radius $r = 17{\cdot}2$ cm, angular aperture $\alpha = 3{\cdot}89°$ and parallel slit assembly apertures $\delta = 4{\cdot}5°$. Curve 1: Corrections for axial divergence, flat specimen and Lorentz–polarization and dispersion effects. Curve 2: Same corrections plus the transparency correction for a silicon powder specimen, assuming the density is 55% of the density of solid silicon.

8.1. *Goniometer corrections*

A Norelco diffractometer adjusted accurately for optimum performance (Parrish, Hamacher & Lowitzsch, 1954) was used. Careful attention was given to all phases of the alignment in order to eliminate any possibility of asymmetric aberrations caused by cross-term effects (Wilson, 1963). Thus asymmetric aberrations arising from unequal source-specimen-receiving slit distances, misalignment of the primary beam, 2:1 mis-setting, *etc.*, were avoided. A Philips PW1010 D.C. constant potential power supply with good short- and long-range stability and standard Norelco X-ray tubes, with focal line 10 by 0·16 mm at an angle-of-view of 6°, were employed. The same receiving slit, 0·10° (2θ) was used in the angular calibration and subsequent line profile measurements.

To make certain the X-rays entering the counter tube came only from the specimen, an antiscatter slit 2 mm wide was placed behind the receiving slit (in front of the counter tube). The divergence of the primary beam in the axial plane was limited (in addition to the parallel slits) by a 7 mm wide slot built into the constant temperature chamber heat radiation shield. In addition, a broad slit was placed over the scintillation crystal and the X-ray tube housing was carefully shielded to prevent stray and higher voltage X-rays from entering the counter tube at any diffraction angle. These precautions were required to obtain significant background measurements.

Goniometer gear calibration. The goniometer was calibrated at the National Bureau of Standards, Optics and Metrology Section, Washington, D.C., using the precision polygon method (Taylerson, 1947; Haven & Strang, 1953). A calibration curve to correct for slight non-uniformities of the worm gear was thus established and used to correct the angular measurements.

Zero-angle measurement. The deviation of the nominal zero dial reading from the true zero angle of the goniometer was determined by the pinhole method (Parrish & Lowitzsch, 1959) after the goniometer had been aligned for a 6° angle-of-view, and with the 0·10° receiving slit in place. The 2:1 relationship was established accurately at 0° and the 2:1 tracking over the entire angular range was found to be satisfactory with a sensitive dial indicator gauge.

8.2. *Geometric aberrations*

The derivations of the formulas used for the aberration corrections are given by Wilson (1963). Equations (4) to (8) are the expressions used for the centroid corrections in $°2\theta$.

Instrumental aberrations. As a consequence of the careful alignment procedures used, only the flat specimen and axial divergence aberrations were considered. The flat specimen aberration correction was calculated with the numerical factors appropriate to our experimental arrangement,

$$\Delta_{\text{f.s.}}(°2\theta) = \alpha^2 \cot\theta/343.77 \qquad (4)$$

where the angular aperture α in the focusing plane was 3·89° and the goniometer radius $r = 17{\cdot}2$ cm.

The axial ('vertical') divergence aberration correction was calculated from the formula and parameters derived by Pike (1957, 1959) for two sets of parallel slit assemblies, each with full angular aperture $\delta = 4{\cdot}5°$. The source, specimen and receiving slit 'height' = 1 cm so that the expression used was

$$\Delta_{\text{a.d.}}(^\circ 2\theta) = 0{\cdot}01125 \cot 2\theta + 0{\cdot}00188 \csc 2\theta \,. \quad (5)$$

The X-ray tube focal line and receiving slit widths broaden all line profiles symmetrically, and hence no corrections of the centroids are required for these factors.

Specimen aberrations. Relatively thick specimens (about 1·5 mm) were used. The powders were mixed with a small amount of a mixture of 1 part collodion and 10 parts amyl acetate and packed into a rectangular depression machined in a special copper block. The block also contained the heater and temperature-sensing device and will be described elsewhere. The specimens were checked for uniformity with a binocular microscope. The particle sizes of the silicon powder were in the range 5 to 10 μ in diameter and those of tungsten 1 to 10 μ. Hence there were no difficulties in the intensity measurements from too large crystallite sizes (de Wolff, Taylor & Parrish, 1959). The line profiles were narrow and well-shaped and showed no evidence of strain or too small crystallite sizes. The tungsten profiles were about 8% narrower than silicon profiles at nearly the same diffraction angles. The silicon was from the same batch as the I.U.Cr. sample (Parrish, 1960) except that a smaller particle size fraction was used. Spectrographic and chemical analysis of the tungsten sample (Leber, 1961) indicated the following: Co, absent; Na, K, Cr, Ni, Mn, Mg, Sn < 0·001; Cu 0·001; Al, Si 0·002; Fe 0·005; Mo 0·058; O_2 0·203%.

The transparency aberration correction was calculated from

$$\Delta_{\text{tr}}(^\circ 2\theta) = 1{\cdot}6656 \sin 2\theta/\mu_l \quad (6)$$

where μ_l is the linear absorption coefficient of the specimen. The packing density of the silicon specimen was determined experimentally and found to be 55% of the density of solid silicon. This was taken into account in calculating μ_l from the published values of the mass absorption coefficient. The packing density of the tungsten specimen was assumed to be 55% also. If this figure is in error for tungsten, it will have negligible effect on the transparency correction which is extremely small.

The specimen surface displacement aberration correction was found using the formula

$$\Delta_{\text{s.d.}}(^\circ 2\theta) = 6{\cdot}6623\, S \cos\theta \quad (7)$$

where S is the surface displacement in cm. The displacement was measured by a mechanical method (unpublished) and checked optically, and was essentially zero for the silicon specimen, and 0·0005 cm outside the focusing circle for the tungsten specimen.

8.3. *Physical aberrations*

Lorentz, polarization and dispersion. The corrections for these factors, Δ_L were calculated from the expression (Pike & Ladell, 1961)

$$\Delta_L(^\circ 2\theta) = \frac{180}{\pi} \times \left[-\frac{V}{\lambda_C^2} \tan^3\theta \left\{ 3 - 4\cot^2\theta - \frac{16\cos 2\theta \cos^2\theta}{1+\cos^2 2\theta} \right\} \right] \quad (8)$$

where V is the variance, λ_C the centroid of the spectral distribution, and θ is the Bragg angle. The Bearden 1960 spectral distributions (Mack, Parrish & Taylor, 1964) were used to obtain both V and λ_C for various integration ranges. The range dependence can be seen in Table 2 where Δ_L for Fe $K\alpha$ is given for three ranges. The variation of Δ_L with range for Cu $K\alpha$ is too small to be significant here.

In method A, the ranges on the spectral and powder profiles for a given value of P are not equivalent, and in fact the kX range for a given P varies from reflection to reflection. Hence to derive Δ_L for method A centroids, each powder reflection would have to be treated individually. This has not been done since A does not satisfy the requirements of a good truncation procedure, and Δ_L is given in Table 2 for methods C and D only.

Refraction. While each centroid could be corrected for refraction (Wilkens, 1960), it is more convenient to correct the final lattice parameter. For cubic crystals, the expression is

$$(1-n)a = 4{\cdot}47 \times 10^{-6} (\lambda/a)^2 \Sigma A \quad (9)$$

where n is the refractive index, a the lattice parameter, λ the wavelength, and ΣA the sum of the atomic numbers of the atoms in the unit cell (Wilson & Lipson, 1941). The corrections in kX units applied to the lattice parameters of silicon and tungsten respectively were $+4{\cdot}0 \times 10^{-5}$ and $+15{\cdot}7 \times 10^{-5}$ for Cu $K\alpha$ and $+6{\cdot}4 \times 10^{-5}$ and $+24{\cdot}7 \times 10^{-5}$ for Fe $K\alpha$.

Temperature correction. The temperature chamber held the specimen temperature to $\pm 0{\cdot}2$ °C. The profiles used for centroid determination were measured at 38·2 °C. Using peak measurements, the thermal coefficient of expansion α was determined at 38·2, 78·2, and 98·2 °C and was linear over this range. The values of α obtained were $2{\cdot}7 \times 10^{-6}$ for silicon and $4{\cdot}4 \times 10^{-6}$ for tungsten. The lattice parameters measured at 38·2 °C were corrected to 25·0 °C using the relation

$$a_{T_2} = a_{T_1}[1 + \alpha(T_2 - T_1)] \quad (10)$$

where a is the lattice parameter, $T_1 = 38{\cdot}2°$ and $T_2 = 25{\cdot}0$ °C. Thus the temperature correction was $\Delta a = -0{\cdot}00020$ kX for silicon and $-0{\cdot}00018$ kX for tungsten.

8.4. *Response variations*

One of the most difficult problems in the centroid method is to obtain accurate centroid wavelengths. Preliminary values for Cu $K\alpha$ and Fe $K\alpha$ radiations calculated from the Bearden 1960 two-crystal spectrometer profiles were published recently by Mack,

Table 3. *Method D centroid wavelengths* (kX)

	Cu $K\alpha$				Fe $K\alpha$	
			Modified for powder diffr.‡			
R (kX)	Bearden 1960*	Sat. gp. Adj.†	0·0006″ Ni	0·0012″ Ni	Bearden 1960*	Modified§ 0·001″ Mn
0·012	1·5387 84	1·5387 84	1·5387 68	1·5387 60	1·933 566	1·933 534
0·014	92	92	76	68	76	543
0·016	91	90	74	66	81	546
0·018	88	81	65	57	79	541
0·020	86	70	54	46	69	529
0·022					54	511
0·024					43	497
0·026					37	490
0·028					36	488
0·030					36	488

* Mack, Parrish & Taylor (1964). Corrected for aberrations.
† Values of col. 2 adjusted for proper $K\alpha$ satellite group intensity.
‡ Values of col. 3 modified for powder diffractometer experimental conditions given in Table 4.
§ Values of col. 6 modified for powder diffractometer experimental conditions given in Table 4.

Parrish & Taylor (1964). If the experimental conditions employed in the two-crystal spectrometer and the powder diffractometer had been identical, the spectral data could have been used directly. However, since the experimental conditions were different, the spectral data required corrections for differential absorption across the profile caused by the X-ray tube window, air path, detector quantum counting efficiency, β filter, *etc.*, as well as correction for other factors, such as axial divergence and the crystal asymmetry function. Hence the first step was to correct the centroid wavelengths of the Bearden 1960 data to represent the $K\alpha$ spectral distributions emitted at the X-ray tube target*. The corrected centroid wavelengths for method D are given in columns 2 and 6 of Table 3.

The Cu $K\alpha$ wavelengths were adjusted (Table 3, col. 3) because the $K\alpha$ satellite group was virtually absent from the Bearden 1960 Cu $K\alpha$ spectral curve but present in the observed diffractometer powder profiles; for a detailed discussion of the $K\alpha$ satellites see Parrish, Mack & Taylor (1963), and Mack, Parrish & Taylor (1964). To obtain the adjusted values, the moment contributed by the satellite group was added to the corrected Bearden 1960 values. The moment was estimated from a comparison of single-crystal spectral centroids, in which the satellites were present, with the Bearden 1960 two-crystal centroids.

For adaptation to the powder diffractometer case, the corrected Fe $K\alpha$ and adjusted Cu $K\alpha$ spectral centroids were then modified to compensate for the distortion of the spectrum resulting from differential absorption. Listed in Table 4 are the changes in the method D centroid resulting from the powder diffractometer absorbing paths, *viz.* X-ray tube window 0·005″ beryllium + 0·0005″ mica, air path 34 cm, β filter 0·001″ manganese for both specimens with Fe $K\alpha$ and 0·0006″ nickel for silicon and 0·0012″ nickel for tungsten with Cu $K\alpha$, and scintillation counter window 0·005″ beryllium. The NaI.Tl scintillation crystal absorbed 100% of Cu $K\alpha$ and Fe $K\alpha$ (Taylor & Parrish, 1955, 1956). The modified wave-

* No corrections were applied for differences in X-ray tube voltage used by Bearden (15 kV) and us (40 to 50 kV) because the target self-absorption factors were not known with sufficient accuracy.

Table 4. *Changes in method D centroid wavelengths to compensate for differential absorption factors in powder diffractometer**

	$\Delta\lambda \times 10^{-6}$ kX					
	Cu $K\alpha$	Fe $K\alpha$				
Diff. abs. factor	0·012 to 0·020†	0·012†	0·016†	0·020†	0·024†	0·028†
X-ray tube window	−2·4	−4·7	−5·1	−5·9	−6·6	−7·0
Air path	−5·1	−10·4	−11·3	−12·9	−14·6	−15·3
β filter	−8·0 (Si) −16·0 (W)	−16·9	−18·4	−21·1	−23·8	−25·0
Detector window	−0·2	−0·4	−0·4	−0·5	−0·6	−0·6
Total	−15·7 (Si) −23·7 (W)	−32·4	−35·2	−40·4	−45·6	−47·9

* Approximately the same corrections would apply to method C.
† Range in kX.

Table 5. *Method D lattice parameters* (kX), 38·2 °C, *no refraction correction*

(*a*) Silicon, Cu $K\alpha$

	R(kX)							Random error
	0·0125	0·0145	0·0160	0·0180	0·0200	0·0225	0·0250	$\pm\Delta a \times 10^{-5}$
hkl								
444	*5·420 07*	10						1·0
533	*07*	11	12					2·2
620	*14*	21	22	22				2·7
531	*10*	18	20	20	22			3·3
440	*05*	11	14	18	15			3·7
511	02	*08*	11	13	13	17	17	4·2
422	01	08	*07*	09	10	15	15	4·5

$\bar{a}_{R_{\min}} = 5{\cdot}420\ 08 \pm 0{\cdot}0005\,\%$
$\bar{a}_{R_{\text{opt}}} = 5{\cdot}420\ 16 \pm 0{\cdot}0009\,\%$

(*b*) Silicon, Fe $K\alpha$

	0·0125	0·0145	0·0160	0·0180	0·0210	0·0250	
511	*5·419 85*	87	86	88	90		1·9
422	83	*85*	85	87	86	86	2·4
331	78	81	*85*	87	89	89	3·1
400	85	88	88	*87*	90	92	3·4

$\bar{a}_{R_{\min}} = 5{\cdot}419\ 86 \pm 0{\cdot}0002\,\%$
$\bar{a}_{R_{\text{opt}}} = 5{\cdot}419\ 89 \pm 0{\cdot}0005\,\%$

(*c*) Tungsten, Cu $K\alpha$

	0·0125	0·0145	0·0160	0·0175	0·0190	
400	*3·159 12*	13	13			0·8
321	*11*	15	16	16		1·5
222	*08*	11	12	14		1·9
310	*09*	13	17	15	16	2·3
220	01	*05*	05	09	10	2·6

$\bar{a}_{R_{\min}} = 3{\cdot}159\ 09 \pm 0{\cdot}0009\,\%$
$\bar{a}_{R_{\text{opt}}} = 3{\cdot}159\ 14 \pm 0{\cdot}0007\,\%$

(*d*) Tungsten, Fe $K\alpha$

	0·0125	0·0145	0·0160	0·0185	0·0210	0·0250	
310	*3·158 91*	91	90				0·7
220	92	*93*	92	94	92	91	1·5
211	86	87	*87*	88	90	91	1·9

$\bar{a}_{R_{\min}} = 3{\cdot}158\ 90 \pm 0{\cdot}0008\,\%$
$\bar{a}_{R_{\text{opt}}} = 3{\cdot}158\ 91 \pm 0{\cdot}0002\,\%$

lengths, which correspond to those seen by the detector, are given in columns 4, 5 and 7 of Table 3.

Non-linear response of the detector system would depress the $K\alpha_1$ peak more than the $K\alpha_2$ peak and thus cause the calculated centroid of the doublet to be too high. The resolving time of the system was 1 μsec and difficulties from non-linear response were avoided by lowering the X-ray tube current for those profiles in which the $K\alpha_1$ peak intensity exceeded 5000 counts sec^{-1}.

Because the differential absorption corrections are range-dependent, the lack of equivalence between the method *A* spectral and powder ranges introduces the same difficulties in applying the differential absorption corrections as were encountered in applying Δ_L. The adjustment of the Cu $K\alpha$ method *C* spectral centroids for the absence of the $K\alpha$ satellite group is hampered by the horizontal truncation and has not been attempted. For these reasons, and other difficulties previously cited, methods *A* and *C* centroid wavelengths are not given here.

9. Lattice parameter results

The random error in the measurement of the centroid angles was of the order of $\pm 0{\cdot}001°$ (2θ) for the experimental techniques used in this study. The corresponding error in the lattice parameter, $\Delta a = -a \cot\theta \Delta\theta$, is given for each reflection in the last column of Table 5. This high angular precision was required for an evaluation of the effectiveness of the centroid method in eliminating systematic error and can be achieved only with careful attention to all phases of the measurements.

Lattice parameters of silicon and tungsten were calculated with the corrected powder centroids obtained by method D and the appropriate modified wavelengths. Results for a number of ranges for Cu $K\alpha$ and Fe $K\alpha$ are given in Table 5. The last value in each row is $a_{R_{opt}}$, the lattice parameter obtained using an optimum range R_{opt}. R_{opt} was established empirically and satisfies the condition that the lattice parameter for ranges greater than R_{opt} is essentially the same as $a_{R_{opt}}$. Thus, R_{opt} is sufficiently large to include virtually all of the aberration distribution within the truncated profile. The use of increasingly shorter ranges $R < R_{opt}$ resulted in a progressive decrease in a; for these cases the centroids have been 'overcorrected' by applying the full aberration correction. Ideally, a partial aberration correction should be used for these ranges because the truncated profile excludes a portion of the aberration function, but this has not been attempted because of the complexities involved. The magnitude of the error introduced depends on the shape, asymmetry, and relative contribution to the truncated line profile of the aberration function.

There is no *a priori* way of quantitatively determining the optimum range without knowledge of the complete aberration distributions. Qualitatively, the optimum range (in kX) increases as the Bragg angle decreases and the aberration functions become increasingly dominant. We have found that for R_{opt} the intensities at the limits are about 1% of the $K\alpha_1$ peak intensity and have used this empirical correlation for arriving at the range requirements for method D. An estimate of the magnitude of the truncation error resulting from the use of too small a range may be obtained from Table 5 by comparing for each reflection the value of $a_{R_{opt}}$ with the italicized value. The italicized values, $a_{R_{min}}$, were derived using 'minimum' ranges for which the intensities at the limits were about 2% of the $K\alpha_1$ peak intensity.

The mean values $\bar{a}_{R_{min}}$ and $\bar{a}_{R_{opt}}$ and the relative per cent standard derivation given in Table 5 were calculated from the usual relations,

$$\bar{a} = \Sigma f_i a_i / N \tag{11}$$

and

$$\sigma = \sqrt{\frac{\Sigma f_i (a_i - \bar{a})^2}{N-1}} \tag{12}$$

where a_i are the values from the various reflections, f_i are the weighting factors taken as 1 because the a_i are assumed to have equal weight, N is the number of reflections measured, and σ is the standard deviation. The value of $\bar{a}_{R_{min}}$ is significantly smaller than $\bar{a}_{R_{opt}}$, but in both cases the a_i show the same absence of systematic errors. The absence of systematic error was thus a necessary but not sufficient criterion to use in evaluating the data.

The mean method D lattice parameters $\bar{a}_{R_{opt}}$ at 25 °C, corrected for refraction, are given in Table 6(a). The relatively poor agreement (0·004%) between the lattice parameters obtained with Cu $K\alpha$ and Fe $K\alpha$ we ascribe to inaccuracies in the absolute values of the centroid wavelengths, for there was good agreement between lattice parameters obtained from the same data using the peak as the measure of diffraction angle. The peak results and a discussion of the difficulties associated with peak measures are given elsewhere (Parrish, Taylor & Mack, 1964). When more reliable spectral data become available, it will be a simple matter to recompute the centroid lattice parameters and it is expected that the agreement will improve.

Table 6. *Lattice parameters* (kX), 25 °C, *corrected for refraction*

(a) Method D

Radiation	Silicon	Tungsten
Cu $K\alpha$	5·42000	3·15912
Fe $K\alpha$	5·41975	3·15898
% Agreement	0·0046	0·0044

(b) Method C

Radiation	Silicon	Tungsten
Cu $K\alpha$	5·42000	3·15908
Fe $K\alpha$	5·41976	3·15899
% Agreement	0·0044	0·0028

Although methods A, B and C failed to satisfy the theoretical and practical requirements of a good truncation procedure, it should be emphasized that the difficulties involved essentially second-order effects. The individual lattice parameters derived using *all* methods and reasonable ranges agreed to about 0·004% for Cu $K\alpha$ and 0·002% for Fe $K\alpha$ radiation. The mean lattice parameter results derived by the different methods agreed to better than 0·002% for Cu $K\alpha$ and 0·001% for Fe $K\alpha$.

The method C lattice parameters are given in Table 7 to illustrate the internal consistency of that method. The Cu $K\alpha$ wavelengths were not adjusted (see § 8). The mean lattice parameters given in Table 6(b) were calculated from equation (11), using for a_i the last value in the row (Table 7). We have based this choice of a_i on the same considerations described for the determination of $a_{R_{opt}}$ in method D. This is an extension of method C, for although the authors recognized the need for including all of the aberration, they have not stated quantitatively how to satisfy this requirement. The good agreement between the method C and D results is not surprising since for the optimum range the base line in method C is generally parallel to the background line in method D.

The determination of the lattice parameter of tungsten by the centroid method with Cu $K\alpha$ radiation has been recently reported by Delf (1963). The truncation method used was a modification of the 'simplified procedure' of method C. He reported $\bar{a} = 3{\cdot}16519$ Å

Table 7. *Method C lattice parameters* (kX), 38·2 °C, *no refraction correction*

(*a*) Silicon, Cu $K\alpha$

	R(kX)						
	0·0125	0·0145	0·0160	0·0180	0·0200	0·0225	0·0250
hkl							
444	5·41998	1999					
533	1998	2001	2006				
620	2005	2013	2016	2017			
531	1998	2008	2008	2018	2022		
440	1996	2000	2003	2012	2014		
511	1992	1999	1998	2004	2023	2032	2032
422	1992	1997	1996	1999	2011	2022	2025

$\bar{a}_{R_{opt}} = 5{\cdot}420\ 16 \pm 0{\cdot}0021\ \%$

(*b*) Silicon, Fe $K\alpha$

	0·0125	0·0145	0·0160	0·0180	0·0210	0·0250
511	5·41987	87	85	88	90	
422	84	86	85	82	82	87
331	83	80	80	82	91	87
400	88	88	83	84	93	96

$\bar{a}_{R_{opt}} = 5{\cdot}419\ 90 \pm 0{\cdot}0008\ \%$

(*c*) Tungsten, Cu $K\alpha$

	0·0125	0·0145	0·0160	0·0175	0·0190
400	3·15908	910	911		
321	905	909	910	915	
222	899	905	907	910	
320	904	906	910	911	912
220	893	896	898	900	904

$\bar{a}_{R_{opt}} = 3{\cdot}159\ 10 \pm 0{\cdot}0013\ \%$

(*d*) Tungsten, Fe $K\alpha$

	0·0125	0·0145	0·0160	0·0185	0·0210	0·0250
310	3·15891	90	91			
220	92	92	91	94	94	93
211	86	87	84	89	90	93

$\bar{a}_{R_{opt}} = 3{\cdot}158\ 92 \pm 0{\cdot}0003\ \%$

(=3·15880 kX) at 25 °C, using a Cu $K\alpha$ wavelength of 1·541 76 Å (=1·538 65 kX), the weighted mean of the $K\alpha_1$ and $K\alpha_2$ peak wavelengths. The discrepancy of 0·010% between our result with Cu $K\alpha$ ($\bar{a}$= 3·15912 kX) and that of Delf is probably due mainly to the use of different wavelengths. The difference between our centroid wavelength for an 0·020 kX range (1·538 754 kX) and the wavelength used by Delf (1·538 65 kX) is 0·007%. An exact comparison is not possible because there is no relationship between centroid wavelengths and the weighted mean peak wavelength. In addition, the Delf experimental conditions differ in some respects from ours and the ranges used are not specified.

In the centroid method all lines are corrected for systematic errors, and hence in theory any line could be used for a lattice parameter determination. In this study all the $K\alpha$ reflections in the back-reflection region have been measured in order to test the validity of the theory. Normally, the highest angle lines are preferred for lattice parameter determination because a given angular error results in a proportionally smaller error in d, the larger the Bragg angle. However, the reproducibility of the centroid of the highest angle lines, say $>155°$ (2θ), is not as good as for lower angle lines because of the greater background slope and generally lower peak-to-background ratio. In addition, the angular range required becomes excessively large because of the great dispersion, and the corrections Δ_L and $\Delta_{a.d.}$, which increase rapidly in this region and become infinite at 180° (2θ), are difficult to determine accurately. Consequently, it is not certain that the greatest reliance should be placed on the highest angle lines, and indeed our experimental studies indicate that the range from approximately 120° to 150° is preferable.

10. Discussion

The objectives of this research — to determine if the centroid method could properly account for the systematic errors, and to develop a method of accurate lattice parameter determination based on sound theoretical and experimental principles — appear to have been fulfilled. There remains the difficult problem for the X-ray spectroscopists of supplying complete line profile data so that accurate centroid wavelengths can be calculated. This phase of the X-ray wavelength question is in addition to the general problem of converting the kX scale to the metric scale, Since the systematic errors are radiation-dependent, the use of different radiations provides a stringent test of the accuracy of lattice parameter determinations. One cannot claim a greater accuracy for a lattice parameter than the agreement between results obtained with two or more radiations. The agreement of the centroid method results for Cu $K\alpha$ and Fe $K\alpha$ was not as good as expected, probably as a consequence of the limited accuracy of the presently available centroid wavelengths.

We are indebted to Prof. J. A. Bearden, The Johns Hopkins University, Baltimore, for preparing the two-crystal spectrometer spectral curves used for calculating the centroid wavelengths; Prof. A. J. C. Wilson, University College, Cardiff, for helpful discussions; Dr Sam Leber, General Electric Company, Cleveland, Ohio, for the tungsten powder sample; and the following colleagues at Philips Laboratories: Dr J. Ladell and Dr N. Spielberg for helpful discussions, Miss Therese Gendron for computer calculations, and Mrs Phyllis Harnack for aid in the later phases of the data reduction.

References

Bearden, J. A. (1960). Personal communication.
Chipman, D. R. & Paskin, A. (1959). *J. Appl. Phys.* **30**, 1992.
Delf, B. W. (1963). *Brit. J. Appl. Phys.* **14**, 345.
DuMond, J. W. M., Cohen, E. R. & McNish, A. G. (1962). In *Int. Tables for X-ray Cryst.* Vol. III, p. 39. Birmingham: Kynoch Press.
Haven, C. E. & Strang, A. G. (1953). *J. Res. Nat. Bur. Stand.* **50**, 45.
Ladell, J., Parrish, W. & Taylor, J. (1959). *Acta Cryst.* **12**, 561.
Leber, S. (1961). Personal communication.
Mack, M., Parrish, W. & Taylor, J. (1964). *J. Appl. Phys.* **35**, 1118.
Parrish, W. (1960). *Acta Cryst.* **13**, 838.
Parrish, W. (1962*a*). *Advances in X-ray Diffractometry and X-ray Spectrography.* Eindhoven: Centrex Publ. Co.
Parrish, W. (1962*b*). In *Int. Tables for X-ray Cryst.* Vol. III, p. 144. Birmingham: Kynoch Press.
Parrish, W., Hamacher, E. A. & Lowitzsch, K. (1954). *Philips Tech. Rev.* **16**, 123.
Parrish, W. & Kohler, T. R. (1956). *Rev. Sci. Instrum.* **27**, 795.
Parrish, W. & Lowitzsch, K. (1959). *Amer. Min.* **44**, 765.
Parrish, W., Mack, M. & Taylor, J. (1963). *J. Appl. Phys.* **34**, 2544.
Parrish, W., Taylor, J. & Mack, M. (1964). *Advanc. X-ray Analysis* Vol. 7. W. M. Mueller, ed. New York: Plenum Press.
Parrish, W. & Wilson, A. J. C. (1954). *Amer. Cryst. Assoc.* Harvard Univ., Paper A–39, 5 April 1954.
Pike, E. R. (1957). *J. Sci. Instrum.* **34**, 355.
Pike, E. R. (1959). *J. Sci. Instrum.* **36**, 52.
Pike, E. R. & Ladell, J. (1961). *Acta Cryst.* **14**, 53.
Pike, E. R. & Wilson, A. J. C. (1959). *Brit. J. Appl. Phys.* **10**, 57.
Taylor, J., Mack, M. & Parrish, W. (1963). *Acta Cryst.* **16**, 1179.
Taylor, J. & Parrish, W. (1955). *Rev. Sci. Instrum.* **26**, 367.
Taylor, J. & Parrish, W. (1956). *Rev. Sci. Instrum.* **27**, 108.
Taylerson, C. O. (1947). *The Machinist* (*London*) **71**, 1821.
Umanskii, M. M., Kheiker, D. M. & Zevin, L. S. (1959). *Soviet Phys.—Cryst.* **4**, 345.
Warren, B. E. (1959). *Prog. Metal Phys.* **8**, 147.
Wilkens, M. (1960). *Acta Cryst.* **13**, 826.
Wilson, A. J. C. (1962*a*). *Norelco Reporter*, **9**, 55.
Wilson, A. J. C. (1962*b*). Personal communication.
Wilson, A. J. C. (1963). *Mathematical Theory of X-ray Powder Diffractometry.* Eindhoven: Philips Technical Library.
Wilson, A. J. C. & Lipson, H. (1941). *Proc. Phys. Soc.* **53**, 245.
Wolff, P. M. de, Taylor, J. & Parrish, W. (1959). *J. Appl. Phys.* **30**, 63.
Zevin, L. S., Umanskii, M. M., Kheiker, D. M. & Panchenko, YU. M. (1961). *Soviet Phys.—Cryst.* **6**, 277.